Passive Crowd Speed Estimation and Head Counting Using WiFi

***Abstract*—In this paper, we propose a framework to sense occupancy attributes of an area, such as speed of a crowd traversing through the area, the total number of people in the area, and the rate of arrival of people into the area, using only the received power measurements (RSSI) of two WiFi links, and without relying on people to carry any device. We first show that the cross-correlation between the two WiFi link measurements and the probability of crossing a link implicitly carry key information about the occupancy attributes and develop a mathematical model to relate these parameters to the occupancy attributes of interest. Based on this, we then propose a system to estimate the occupancy attributes and validate it with 51 experiments in both indoor and outdoor areas, where up to (and including) 20 people walk in the area with different possible speeds, and show that our framework can accurately estimate the occupancy attributes. For instance, our framework achieves a Normalized Mean Square Error (NMSE) of 0.047 (4.7%) when estimating the speed of a crowd, an NMSE of 0.034 (3.4%) when estimating the arrival rate to the area, and a Mean Absolute Error (MAE) of 1.3 when counting the total number of people. We finally run experiments in an aisle in Costco, showing how we can estimate the key attributes of buyers' motion behaviors.**

I. Introduction

Sensing the occupancy attributes of an area, such as the corresponding speed of people when traversing the area, their arrival/departure rate into/out of the area, as well as the total number of people in the area can be useful in many applications. For instance, retail stores can learn about the popularity of the products in different aisles, if they know buyers' speed/density in different parts of the store. Consider an aisle in a retail store containing a specific type of product, for instance. Shoppers that are entering this aisle will walk at a normal pace if the products in the aisle do not attract their attention. On the other hand, they may slow down, or stop to look at the items if they find them of interest. Therefore, by estimating the average speed of the shoppers in an aisle, the popularity of the products in that aisle can be inferred. This information, in turn, can significantly help with business planning. Similarly, museums can estimate which of their exhibits are more popular, based on the speed of the visitors, as well as their arrival rate into different areas. Smart cities can further design the traffic signal timings for the pedestrian crosswalks based on their speeds [1]. Furthermore, identifying the slow areas can help with city planning by allocating new roads and facilities. Public places, such as a train station, on the other hand, can further detect abnormal behaviors if an atypical slow down is detected in a particular area. Resources can then be allocated accordingly.

In this paper, we propose a framework that can estimate the **occupancy attributes of an area, including the speed of a crowd when traversing the area, the arrival/departure rate into/out of the area, or the total number of people in the area**, using only the received signal strength (RSSI) of two WiFi links in the area of interest, **and without relying on people to carry any device (i.e., passively)**. Since a person may not have a constant speed in an area, in this paper **"speed estimation" refers to estimating the *average speed* of the people, where the average is the spatial average of the speed of a person in that particular area.**[1] In other words, people can stop several times in an area, or change their instantaneous speed. We are then interested in estimating their average speed, which is area-dependent and can thus reveal valuable information about an area.

To keep the paper applicable to many scenarios, we consider two possible general cases, as shown in Fig. 1. The first case (Fig. 1(a)), can represent a museum, a conference, or an exhibit-type setting where the total number of people inside the overall area changes slowly with time such that it can be considered constant over a small period of time. People can have any motion behavior in this area and can possibly traverse the area several times back and forth, depending on their interest. We refer to this case as the **closed area** case. The second case (Fig. 1(b)), on the other hand, captures the cases where people can enter and exit through both ends, and can form flow directions through the area. Then the total number of people can change rapidly with time and cannot be considered a constant. This case represents scenarios like train stations or a store aisle. We then refer to the second case as the **open area** case. As we shall show in this paper, the estimation of occupancy attributes can be achieved under the same unifying framework for both cases, by estimating the rate of arrival of people for the open case, and the total number of people in the area (over a small period of time) for the closed case.

A. Related Work

We next discuss the state-of-the-art on estimating the occupancy attributes of an area.

1) **Infrared-Based Approaches:** Infrared (IR) sensors are mainly used for occupancy detection by sensing the motion of the occupants [2]–[4]. IR sensors located at the entrances/exits can also count the number of people entering and exiting the area [5], [6]. Recently, IR sensors are also used to estimate the number of people in an area, without relying on door counters [7]. However, they are limited to counting up to 8 people in the area. More recent work also classifies the walking speed of a single person in an area based on IR sensors [6], [8]. However, there is no work based on IR sensors that can estimate the speed of a crowd (i.e., estimate the speed beyond one person), or count the number of people in an open setting, or count beyond 8 people for the closed case.

2) **Vision-Based Approaches:** Vision-based methods can be potentially used to estimate the occupancy attributes of

[1] We may drop the term "average" throughout the paper for brevity.

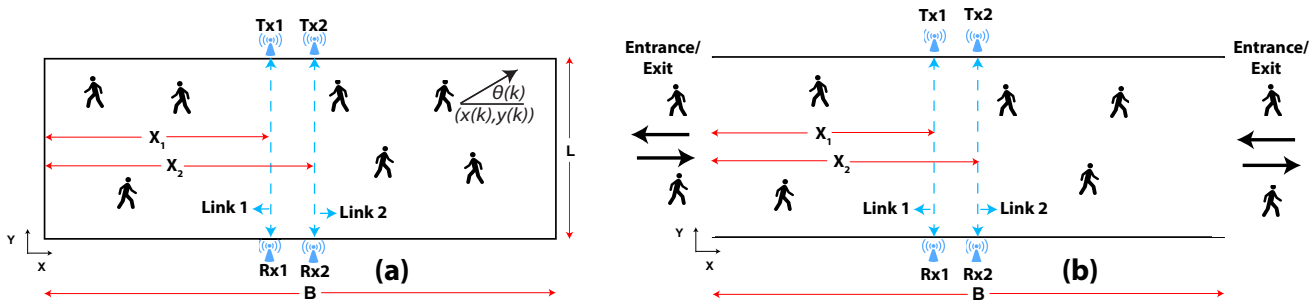

Fig. 1: Two example scenarios of the problem of interest, (a) a closed and (b) an open area. A pair of WiFi links are located in the area. We are then interested in estimating the occupancy attributes of the area, based on only WiFi RSSI measurements of the links. (a) shows an example of a closed area, such as an exhibition or a museum, where the total number of people inside the area changes slowly with time and people can traverse back and forth or change directions inside the area any number of times depending on their interest. For a closed area, we are then interested in estimating the total number of people in the area and their walking speed, (b) shows an example of an open area such as a train station, where people can come and go from both sides and can form flow directions. In this scenario, we are then interested in estimating the walking speed and the rate of arrival of people into the area.

an area [9]–[13]. This involves continuous recording of an area, using cameras, followed by computer-vision algorithms for processing the videos. However, while consumers are fine with security cameras being probed in an on-demand manner for security purposes, serious privacy concerns arise when cameras are utilized in public places to analyze customer behaviors. For instance, a recent survey on retail shoppers [14] revealed that 75% of the people who understood the capabilities of vision-based tracking technologies found it intrusive for retails to track their behavior using such a technology. Furthermore, employing such tracking techniques could lead to shoppers choosing not to visit the corresponding stores [15]. In summary, vision-based occupancy estimation methods have the major drawback of privacy violation. Furthermore, they can only estimate the occupancy attributes in the areas that are in the direct line-of-sight of the cameras, while Radio Frequency (RF) based approaches have a through-wall sensing capability.

3) **Device-based Active RF Approaches:** The device-based active methods depend on the RF signals transmitted from a device carried by people in the area to assess the occupancy attributes [16]–[18]. However, these methods require the shoppers to carry a wireless device, or an on-body sensor, which limits their applicability. More importantly, if a store is to use shoppers' devices to gather store analytics, it can only gather crude, low resolution tracking data, based on monitoring which router the device is connected to in the store (e.g., this data may not directly translate to speed estimation in different aisles). Even then, serious privacy concerns limit the applicability of such an approach in public places. For instance, Nordstrom, a clothing company which implemented an active WiFi-based in-store tracking technology to analyze the behavior of their customers, withdrew it due to privacy concerns of the shoppers [19]. Furthermore, a recent survey on active WiFi tracking technology [15] revealed that 80% of the shoppers do not like to be tracked based on their smartphones, while 43% do not want to shop at a store that employs active WiFi tracking technology.

4) **Device-free Passive RF Approaches:** The device-free passive methods, on the other hand, leverage the interaction of RF signals with the pedestrians and hence do not require the pedestrians to carry any device. In this manner, they can preserve the privacy. For instance, [20]–[22] use the variations in the WiFi RSSI signals, caused by people, to estimate the number of people. [23] uses channel state information (CSI) measurements and its corresponding variations for counting. However, these methods rely on extensive prior calibrations to the extent of running an actual experiment with several people walking in the area. They further require several wireless links, and are focused on closed areas only (i.e., cannot handle time-varying number of people in the area). [24] estimates the number of people in an area by minimizing the required prior calibration. However, they have to assume the speed of the people, and further only focus on the closed-area case. In terms of speed estimation, some recent work started to estimate the speed of people in a device-free manner. For instance, [25] estimates the speed of a single person walking in a circle of radius 2 m, based on the RSSI measurements of a mobile phone located at the center of the circle. [26] classifies the speed of a single person based on the FM radio receivers. However, all these methods require an extensive prior training phase and are limited to a single person. In [27], RSSI measurements of several WiFi links are used to track up to 4 people walking in the same area. Such an approach can in principle be extended towards speed estimation. However, this and other work on tracking typically have to assume very few people (less than 5). Moreover, in order to estimate the speed of a crowd of pedestrians, there is no need to track every individual, as we shall see in this paper. In summary, to the best of our knowledge, there is no work in the literature that can estimate the speed of a crowd passively. Furthermore, there is no work that can jointly estimate the speed and total number/rate of arrival of people.

In this paper, we propose a system to estimate both the crowd speed and crowd count (i.e., total number of people for the closed case and arrival rate to the area for the open case), passively, and by using only a pair of WiFi links in the area. We next summarize our main contributions.

- We mathematically characterize the cross-correlation between the two WiFi link measurements and show that it contains key information about the crowd speed in the area.
- We mathematically characterize the probability of crossing a link and explicitly show its dependency on the total number of people for the closed case, and on the rate of arrival of

people for the open case. Our mathematical characterization is general in the sense that it can include any type of motion patterns dictated by the environment.

- We implement a framework to estimate the crowd speed, number of people, and rate of arrival of people in an area, using a pair of WiFi links, and validate its performance using a total of 51 experiments, in both indoor and outdoor areas, for both open and closed cases, and with up to (and including) 20 people, and show that our framework can accurately estimate the occupancy attributes of an area in a device-free passive manner. **To the best of our knowledge, this is the first demonstration of passive crowd speed estimation, as well as the first demonstration of passive joint estimation of crowd speed and count for both open and closed areas.**
- We deploy our framework in an aisle of a local retail store, Costco, and estimate the behavior of shoppers in the aisle.

The rest of the paper is organized as following. In Section II, we mathematically characterize two key statistics, the cross-correlation between two WiFi links, and the probability of crossing a link, and show how they carry vital information on the crowd speed and number of people/arrival rate, and propose a methodology to estimate them accordingly. In Section III, we thoroughly validate our framework with 51 experiments where up to 20 people walk in both indoor and outdoor areas, and for both closed and open scenarios. We further test our methodology in Costco. We conclude in Section IV.

II. Proposed Methodology and System Design

In this section, we propose a system to estimate the occupancy attributes of an area, i.e., the speed of a crowd as well as the total number (or arrival rate for the open case), using only a pair of WiFi links, as shown in Fig. 1. More specifically, we first show that the cross-correlation between the two links is mainly a function of the crowd speed. We next derive a mathematical expression for the probability of pedestrians crossing a WiFi link. Our analysis shows that these parameters carry key information on the speed/number of the pedestrians, which we then use to estimate the occupancy attributes. We next start by summarizing a probabilistic model to capture the motion dynamics of a casual walk in the area, followed by discussing how occupants affect the received signal power.

A. Pedestrian Motion Model

In this paper, we extend the pedestrian motion model developed in [24], which captures casual walking patterns, to more general cases where environmental characteristics can also be captured.

Consider the motion of a single person in the workspace. Let $x(k)$, $y(k)$, and $\theta(k)$ denote the position along x-axis, the position along y-axis, and the heading of the person w.r.t. the x-axis, at time k, respectively, as marked in Fig. 1(a). In a casual walk, a person keeps walking in a particular direction while occasionally changing his/her direction. This walking pattern can then be captured by the following model:

$$\theta(k+1) = \begin{cases} \theta(k) & \text{with probability } p \\ \text{Uniformly in } \mu & \text{with probability } 1-p. \end{cases} \quad (1)$$

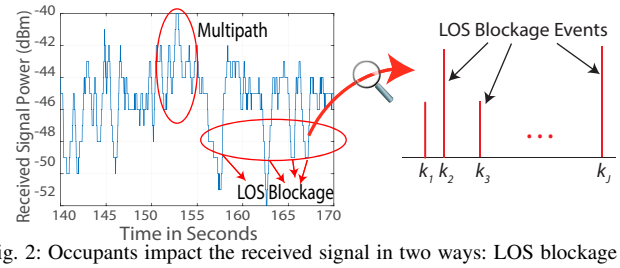

Fig. 2: Occupants impact the received signal in two ways: LOS blockage and multipath, samples of which are marked on the figure. It can be seen that the LOS blockage results in more significant attenuations of the wireless measurements, as compared to the fluctuations induced by the multipath. We use the LOS blockage event sequence obtained from the wireless measurements to estimate the occupancy attributes.

For the case of Fig. 1(a), people can change their direction any time and can traverse the area back and forth as many times as they wish. Thus, we have $\mu = [-\theta_{\max},\ \theta_{\max}] \cup [\pi - \theta_{\max},\ \pi + \theta_{\max}]$, to capture this behavior. $\theta_{\max}$ then defines the maximum angle for the direction of motion, and is an environment-dependent parameter. For instance, in long hallways, people may have a pattern more close to a straight line, resulting in a smaller $\theta_{\max}$, while in a supermarket, people may often deviate from a straight line to check out grocery items. Parameterizing the motion model with $\theta_{\max}$ then allows us to capture the characteristics of different environments. For this closed-area case, we assume that when a person encounters any of the four boundaries of the area, she/he reflects off of the boundary, similar to a ray of light.[2]

For the case of open area of Fig. 1(b), on the other hand, we assume that people walk mainly in the forward direction, entering from one end, and exiting from the opposite end of the area. Such a motion behavior can characterize the motion in many open areas, such as exhibitions and aisles. Thus, we take $\mu = [-\theta_{\max},\ \theta_{\max}]$ or $\mu = [\pi - \theta_{\max},\ \pi + \theta_{\max}]$ depending on the direction of motion.

Based on Eq. (1), the position dynamics are then given as follows for both open and closed cases:

$$\begin{aligned} x(k+1) &= x(k) + v\delta t\ \cos(\theta(k)) \\ y(k+1) &= y(k) + v\delta t\ \sin(\theta(k)), \end{aligned} \quad (2)$$

where δt is the time step and v is the walking speed.

B. Effect of Pedestrians on Wireless Links

The occupants affect a link in two major ways: (i) Line of Sight blockage effect and (ii) multipath effect. More specifically, when a pedestrian blocks the LOS link, the received signal strength drops significantly, to which we refer as Line of Sight blockage effect. When the pedestrian is not along the LOS path, on the other hand, she/he can act as a scatterer, reflecting the transmissions from the Tx to the Rx, causing fluctuations in the received signal, a phenomena known as the multipath fading effect. Fig. 2 shows the impact of LOS blockage and MP effects on the received wireless signal as people walk in the area. As can be seen in the figure, LOS blockage attenuates the received signal considerably while the MP effect results in less significant fluctuations in the wireless

[2]This boundary behavior is only assumed for the purpose of modeling. In our experiments, we have no control over how people walk.

signals. Our proposed methodology of this paper relies on the LOS blockage events. Thus we first extract the LOS blockage event sequence from the RSSI measurements, as shown in Fig. 2. In Section III-A2, we show how to estimate the LOS blockage sequence from the RSSI measurements.

C. Cross-correlation to Estimate the Crowd Speed

In this section, we propose to use the cross-correlation between the LOS event sequences, corresponding to the two WiFi links, and show that it contains implicit information about the walking speed of the pedestrians in an area.

Consider the closed area of Fig. 1(a). Let $Y_1(k)$ and $Y_2(k)$ denote the event sequences corresponding to Link 1 and Link 2, as defined below:

$$Y_i(k) = \begin{cases} l & \text{if } E_l \text{ happens at time } k \\ 0 & \text{otherwise} \end{cases}, \text{ for } i \in \{1, 2\},$$

where E_l denotes an event corresponding to l people blocking the LOS path. Fig. 2 shows a sample LOS blockage event sequence. The cross-correlation between the two event sequences, $Y_1(k)$ and $Y_2(k)$, is then given by

$$R_{Y_1Y_2}(\tau, v) = \frac{\text{Cov}\Big(Y_1(k), Y_2(k+\tau)\Big)}{\sqrt{\text{Var}\Big(Y_1(k)\Big)\text{Var}\Big(Y_2(k+\tau)\Big)}}, \quad (3)$$

where Cov(. , .), and Var(.) denote the covariance and variance of the arguments, respectively. Since the pedestrians walk independent of each other, we have,

$$Y_i(k) = \sum_{j=1}^{N} Y_i^j(k), \text{ for } i \in \{1, 2\}, \quad (4)$$

where $Y_i^j(k) = 1$ if the j^{th} person blocks Link i at time k, and is 0 otherwise, for $i \in \{1, 2\}$. N is the total number of people in the area, which we take to be constant over the estimation period for the closed case.

Lemma 1. *The cross-correlation, $R_{Y_1Y_2}(\tau, v)$, between the event sequences $Y_1(k)$ and $Y_2(k)$ is a function of only the speed of the people v in the area and is independent of the number of people in the area for the case of closed area.*

Proof. Consider the closed area of Fig. 1(a). Since we assume independent motion for the pedestrians, it can be easily confirmed that the numerator and the denominator of Eq. (3) are proportional to N, resulting in the cross-correlation becoming independent of N. This can be seen by substituting Eq. (4) in (3), and further simplifications, which results in

$$R_{Y_1Y_2}(\tau, v) = \frac{\text{Prob}(Y_2^j(k+\tau) = 1 | Y_1^j(k) = 1) - p_{c,\text{single person}}}{1 - p_{c,\text{single person}}}, \quad (5)$$

for any $j \in \{1, 2, \cdots, N\}$, where $p_{c,\text{single person}}$ denotes the probability of crossing a link by a single person. While it is considerably challenging to derive a closed-form expression for the cross-correlation, the dependency on the crowd speed can be easily seen. For instance, the first term in the numerator of Eq. (5), $\text{Prob}(Y_2^j(k+\tau) = 1 | Y_1^j(k) = 1)$, is the probability that the j^{th} person is at Link 2 at time $k+\tau$, given that she/he is at Link 1 at time k. Clearly this depends on the speed at which the j^{th} person is walking. Hence the cross-correlation in Eq. (5) contains information about the speed of the pedestrians. □

Lemma 2. *For the case of the open area, the cross-correlation $R_{Y_1Y_2}(\tau, v)$ is a function of only the speed of the people v and is independent of the rate of arrival, when the arrivals follow a Poisson process.*

Proof. The Lemma can be proved after a few lines. We skip the proof due to space limitations.

For the case of open area of Fig. 1(b), deriving an expression for the cross-correlation, for a general arrival process distribution is considerably challenging. However, our extensive simulations with various speed and arrival rate combinations show that the cross-correlation is mainly a function of the speed of the people in the area.

The strong dependency of the cross-correlation on the crowd speed, for both open and closed cases, then allows us to devise a simple low-complexity approach for estimating it. More specifically, we simulate a single person walking in the area, according to the motion dynamics in Eq. (2) and with different possible speeds, and generate the event sequences corresponding to the two links in the area. We then generate a database for the cross-correlation function $R_{Y_1Y_2}(\tau, v)$ for a range of walking speeds v. Since the cross-correlation is independent of the number of people in the area, the database for $R_{Y_1Y_2}(\tau, v)$, obtained with 1 person walking in the area (or one rate of arrival for the open case), is valid for any number of people in the area. This makes the database generation a one-time and low complexity operation. The walking speed in an area is then estimated by matching the cross-correlation with the database as follows:

$$\widehat{v} = \min_{v} \sum_{\tau=0}^{\tau=T} \Big(R^{\text{exp}}_{Y_1,Y_2}(\tau) - R_{Y_1,Y_2}(\tau, v)\Big)^2, \quad (6)$$

where $R^{\text{exp}}_{Y_1,Y_2}(\tau)$ is the cross-correlation between the two event sequences obtained during the real experiment.

D. Characterization of the Probability of Crossing

To build a complete picture of occupancy attributes, we next show that the pair of links can also estimate the total number of people or their arrival rate to the area as well. We first characterize the probability of crossing for the case of the closed area of Fig. 1(a), the analysis of which is more involved since a person can reverse the direction of motion anytime and can bounce back and forth in the area as many times as he/she wishes. We then show how to extend the analysis to the case of open area of Fig. 1(b), putting everything under one unifying umbrella. A key feature of our analysis is using a generalized motion model where different motion behaviors can be captured through the parameter θ_{max} of Section II. We then show how to derive a mathematical expression for the probability of crossing a link, under this motion model.

1) Head Counting for the Case of Closed Area: Consider Fig. 1(a) and the motion model of Eq. (2). Since the heading, and the positions along the x-axis and y-axis at time $k+1$, depend only on the corresponding values at time k, we use a Markov chain model to describe the motion dynamics of each

pedestrian. We then use the properties of the corresponding Markov chain to mathematically derive the probability of crossing a given link by a single pedestrian and show its dependency on the walking speed of the pedestrian. This is then followed by characterizing the probability that any number of people cross a given link, and showing its dependency on the total number of people and their speed.

For the purpose of modeling, we discretize the work-space and assume that people can choose only discrete positions along x-axis, y-axis, and the heading direction.[3] More specifically, $\theta(k) \in \mu^d = \{-\theta_{\max},\ -\theta_{\max}+\Delta\theta,\ \cdots,\ \theta_{\max}\} \cup \{\pi - \theta_{\max},\ \pi-\theta_{\max}+\Delta\theta,\ \cdots, \pi+\theta_{\max}\}$, $x(k) \in \{0,\ \Delta x,\ \cdots,\ B\}$, and $y(k) \in \{0,\ \Delta y,\ \cdots,\ L\}$, where $\Delta\theta$, Δx, and Δy denote the discretization step size for heading and position along x-axis and y-axis respectively. Let N_θ denote the number of discrete angles for the heading.

Let $\Theta(k)$ denote the random variable representing the heading of a pedestrian at time k. Let $\pi^\theta(k)$ represent the corresponding probability vector with the i^{th} element $(\pi^\theta(k))_i = \text{Prob}(\Theta(k) = (\mu^d)_i)$, where Prob(.) is the probability of the argument, and $(\mu^d)_i$ denotes the i^{th} element of the set μ^d. Then from Eq. (1), we have the following Markov chain for the heading $\Theta(k)$:

$$\pi^\theta(k+1) = \pi^\theta(k) P^\Theta, \tag{7}$$

where P^Θ is the probability transition matrix for the heading with $(P^\Theta)_{ij} = \text{Prob}(\Theta(k+1) = (\mu^d)_j | \Theta(k) = (\mu^d)_i)$ and is given by $(P^\Theta)_{ij} = \delta(i-j) \times p + \frac{1-p}{N_\theta} = (P^\Theta)_{ji}$, where $\delta(.)$ is the Dirac-delta function, $N_\theta = \text{card}(\mu^d)$, and card(.) denotes the number of elements in the argument. Since the probability transition matrix P^Θ is symmetric, it is a doubly-stochastic matrix, which implies a uniform stationary distribution for $\Theta(k)$ [28]. This implies that the probability that a pedestrian heads in any given direction (in μ^d) is the same asymptotically.

Let $X(k)$ denote the random variable representing the position of a pedestrian along the x-axis at time k. Similar to the heading direction, we can describe the dynamics of $X(k)$ using a Markov chain. Let P^X denote the corresponding probability transition matrix for $X(k)$. Similar to the heading dynamics we can show that the stationary distribution of $X(k)$ and $Y(k)$ are uniform [24]. We next use these properties of the motion dynamics to derive the probability that a pedestrian crosses the LOS path.

We say that a pedestrian crosses/blocks a given link[4] located at X_i along the x-axis, at time $k+1$, if either $x(k+1) \geq X_i$ and $x(k) \leq X_i$ or $x(k+1) \leq X_i$ and $x(k) \geq X_i$. Consider Fig. 1(a) and the motion model of Eq. (1)-(2). Consider a time interval T, discretized to δt. We then define the probability of crossing link i as follows:

$$p_c = \text{Number of blockage events in time interval [0 T]} \times \frac{\delta t}{T}$$

[3]This is only for the purpose of mathematical characterization. In practice, the position and heading of the pedestrians are naturally not limited to these discrete values.

[4]In this paper, we consider WiFi links that are located parallel to the y-axis (see Fig. 1). However, the derivation of the probability of crossing can be extended to any general link configuration following a similar approach.

We then have the following theorem for the probability of crossing a link by a single pedestrian.

Theorem 1. *The probability of crossing a link by a single pedestrian in the area is given by* $p_{c,\text{single person}} = \frac{v\delta t\ \text{sinc}(\theta_{\max})}{B}$, *where* $\text{sinc}(\theta_{\max}) \triangleq \frac{\sin(\theta_{\max})}{\theta_{\max}}$ *with* $\theta_{\max}$ *in radians.*

Proof. See the appendix for the proof of this Theorem.

We next consider the probability of crossing when there are N people in the area. Since, we assume that people in the area walk independent of each other, the probability of crossing, p_c is given as $p_c(N, v) = 1 - (1 - p_{\text{c, single person}})^N$. The number of people in the area can then be estimated as follows:

$$\widehat{N} = \min_N (p_c(N, \widehat{v}) - p_c^{\text{exp}})^2, \tag{8}$$

where $p_c^{\text{exp}} = \frac{p_{c,1}^{\text{exp}} + p_{c,2}^{\text{exp}}}{2}$ and $p_{c,i}^{\text{exp}}$ for $i \in \{1, 2\}$, is the probability of crossing corresponding to Link i obtained from the experiment.

Remark 1. If $\theta_{\max}$ is assumed $90°$, the derivation of Theorem 1 simplifies to the expression derived in [24]. Theorem 1 then generalizes the derivation of p_{cross} to accommodate any $\theta_{\max}$, thus making it applicable to any environment.

2) Rate of Arrival Estimation for the case of Open Area: Consider the scenario of Fig. 1(b) in which people can enter/exit from either side of the area as marked. In this case, the number of people in the area changes with time and hence it is a random variable. As we discussed in Section II-C, the cross-correlation is mainly a function of the speed of people, and thus Eq. (6) can be utilized to estimate the speed of the pedestrians for both open and closed areas. However, we need to extend the probability of crossing analysis to the case of time-varying number of people in order to estimate the rate of arrival to the area, as we show in this part.

Let λ denote the rate of arrival of people into the area (from both ends). In scenarios modeled by the open area, such as a retail store, people typically enter an aisle, spend a random amount of time in the area depending on their interest, before exiting it. Therefore, assuming that the rate of departure is the same as the rate of arrival λ is a reasonable assumption. Furthermore people typically walk mainly in the forward directions rarely turning back. Under these assumptions, the probability of crossing a link in the area can be related to the rate of arrival into the area as follows:

$$p_c = \text{Number of events in time interval [0 T]} \times \frac{\delta t}{T} = \lambda \delta t.$$

We then estimate the rate of arrival, λ, from the crossing probability of each WiFi link as $\widehat{\lambda} = \frac{p_{c,1}^{\text{exp}} + p_{c,2}^{\text{exp}}}{2\delta t}$.

III. Performance Evaluation

In this section, we evaluate the performance of our proposed system using extensive experiments. We start with several experiments in closed areas, where different number of people (up to 20) walk with a variety of speeds, in both indoor and outdoor environments, and show that our proposed approach can accurately estimate the occupancy attributes. In particular, our experiments with 20 people show that our system can estimate occupancy attributes for highly-dense areas. We then

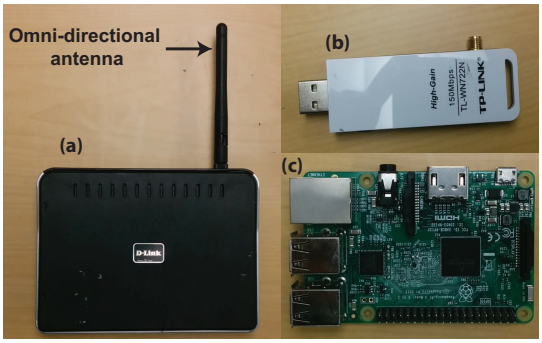

Fig. 3: (a) D-Link WBR 1310 wireless router along with an omni-directional antenna, (b) the TP-Link wireless N150 WLAN card, (c) Raspberry Pi board used to control the data collection process and synchronize the two WiFi links.

show our experimental results for the open-area cases, in both outdoor and indoor environments. Finally, we test our system in a local retail store, Costco, to estimate the rate of arrival and the speed of people in an aisle. Overall, our extensive tests indicate that the proposed approach can accurately estimate the occupancy attributes for both closed and open areas.

A. Experiment Setup

In all our experiments, a pair of WiFi links, located in the area of interest, make RSSI measurements as people walk in the area. Each WiFi link uses a WBR 1310 router as a Tx and a TP-Link wireless N150 WLAN card as a receiver. The Rx of each WiFi link is interfaced with a RaspberryPi (RPI) which controls the data collection operation and stores the corresponding RSSI measurements. Fig. 3 shows the WiFi router, WLAN card, and RPI used in our experiments. This setup is used in all the experiments of the paper. In order to derive the cross-correlation from the experimental data, the receivers of the two WiFi links need to be synchronized in time. To achieve this, we interface the Rx nodes of both WiFi links to the same RPI and program them to receive the wireless signals from their corresponding transmitters at the same time instants. The data is collected at a rate of 20 samples/second at each receiver of the WiFi link. Each link is configured to operate in a different sub-channel of the 2.4 GHz wireless band to avoid any interference. Specifically, we use sub-channel 1, which operates at 2.41 GHz for one link, and sub-channel 13, which operates at 2.47 GHz, for the other link. This separates the two links by the widest frequency margin in the 2.4 GHz WiFi band.

1) Pedestrian Walking Speeds: As shown in Fig 1, our experiments involve different number of people walking at different speeds in the area. We consider three different speeds 0.3 m/s (slow), 0.8 m/s (normal walking), and 1.6 m/s (fast) in our experiments. We ask people to walk casually at a given speed in an experiment. To help people walk at the correct speed, we make use of a mobile application called "Frequency Sound Generator" which generates an audible tone every second. Each person then listens to this application on his/her mobile and takes a step of length v. This ensures correct speeds for people walking in the area. In order to take steps of length v, we have people practice their step lengths to match v prior to the experiments. This procedure is employed only to ensure an accurate ground-truth for the speeds, which is used in assessing the performance of our approach. In our experiments in the aisle of Costco, the speeds of people are naturally determined by their interests in each region, and as such there is no control over peoples' speeds.

2) Separation of LOS from MP: As shown in Section II, our framework is based on the event sequences of a pair of WiFi links located in the area, with the events corresponding to people crossing a WiFi link. Therefore, we need to first extract the event sequences of each WiFi link from the corresponding RSSI measurements. We next describe this process.

To convert the RSSI measurements into an LOS event sequence, we first identify all the dips in the RSSI measurements and the associated times at which the dips occur. Let k_j^i, for $j \in \{1, 2, \cdots, J_i\}$, denote these times for link i, and let $Z_i(k_j^i)$ denote the corresponding RSSI measurement at time k_j^i on link i. The event sequence, $Y_i^{\text{exp}}(k)$, for $i \in \{1, 2\}$, is then obtained from the RSSI measurements as follows:

$$Y_i^{\text{exp}}(k) = \begin{cases} l & \text{if } k = k_j^i \text{ and } Z_i(k_j^i) \text{ is closest to } R_{l,i} \\ 0 & \text{otherwise} \end{cases},$$

where $R_{l,i}$ denotes the RSSI measurement of the i^{th} WiFi link when l people simultaneously block the i^{th} link. We find the values of $R_{l,i}$ by performing a small calibration phase in which l (up to 2) people simultaneously block the i^{th} WiFi link and the corresponding RSSI is measured.[5] Note that small variations in $R_{l,i}$ due to factors such as different dimensions of people crossing the WiFi link have a negligible impact on our results. For instance, we collect $R_{l,i}$ data for only 2 people in the calibration phase, while a total of 10 different people walk in each campus experiment.

B. Experimental Results and Discussion

In this section, we extensively validate our proposed system with several experiments using the aforementioned experiment setup. We first show our results for the case of closed area, followed by the open area, and the retail store results.

Closed Area: Fig. 4 and 5 show the considered outdoor and indoor closed areas of interest respectively. The dimensions of the outdoor area are $B = 14.3\ m$ and $L = 4.26\ m$ and the transceivers are marked on the figure. For the case of indoor, on the other hand, the dimensions are $B = 20\ m$, $L = 2.25\ m$, and the transceivers are marked on the figure. In our first series of experiments, we collect measurements in these areas when 5 and 9 people walk with 3 different speeds in each area (6 different possibilities). Table I then shows the estimates of the occupancy attributes obtained by our system in the outdoor and indoor areas. It can be seen that the proposed system accurately estimates both the number of people and their walking speeds in both indoor and outdoor settings.

To further validate our system statistically, we repeat experiments for each combination of N and v on 3 different days for both the indoor and outdoor areas, running a total of 36 experiments. Table II then shows the normalized mean square

[5]We need to collect this only for small l as the probability of l people simultaneously blocking the LOS link is negligible for higher l.

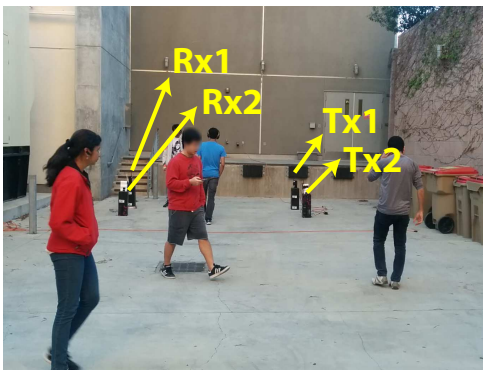

Fig. 4: The outdoor area of interest. The dimensions of the area are $L = 4.26\ m$ and $B = 14.3\ m$. Two WiFi links, each consisting of a transmitter and a receiver, are located in the area, as marked.

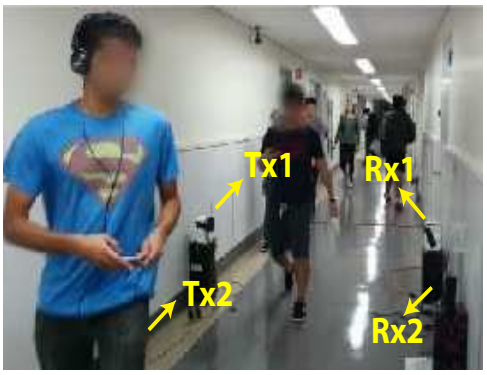

Fig. 5: The indoor area of interest. The dimensions of the area are $L = 4.26\ m$ and $B = 9.76\ m$. Two WiFi links are located in the area, as marked on the figure.

Fig. 6: A snapshot of the experiment when a large number of people (20) are walking in the indoor area of interest.

True Headcount and Speed $(N,\ v)$	**Estimated Headcount and Speed in Outdoor Area** $(\widehat{N},\ \widehat{v})$	**Estimated Headcount and Speed in Indoor Area** $(\widehat{N},\ \widehat{v})$
(5, 0.3)	(5, 0.4)	(6, 0.5)
(5, 0.8)	(4, 0.9)	(4, 1)
(5, 1.6)	(4, 1.9)	(4, 1.6)
(9, 0.3)	(10, 0.4)	(9, 0.5)
(9, 0.8)	(9, 0.9)	(10, 0.9)
(9, 1.6)	(7, 1.9)	(7, 1.9)

TABLE I: Sample performance of our proposed system to estimate the total number and the speed of the people in closed areas – the middle and right columns show the performance for the outdoor area of Fig. 4 and the indoor area of Fig. 5 respectively, while the left column shows the groundtruth.

NMSE of Speed Estimates	**MAE of Headcount Estimates**
0.046 (4.6%)	1.3 person

TABLE II: Average performance (averaged over several trials) in closed areas – the table shows the Normalized Mean Square Error (NMSE) of the speed estimation, and the Mean Absolute Error (MAE) of head counting, based on several experiments in both indoor and outdoor settings.

True Headcount and Speed $(N,\ v)$	**Estimated Headcount and Speed** $(\widehat{N},\ \widehat{v})$
(20, 0.3)	(22, 0.4)
(20, 1.6)	(19, 1.6)

TABLE III: Performance of our system in very crowded areas – the table shows the performance when 20 people walk, with a variety of speeds, in the indoor area of Fig. 6. It can be seen that our approach can estimate the speed and number of people accurately even at high crowd densities.

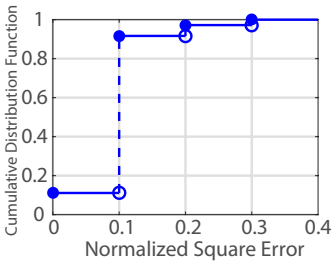

Fig. 7: CDF of the normalized square error for crowd speed estimation in closed areas (both indoor and outdoor). It can be seen that our approach can estimate the crowd speed with a good accuracy.

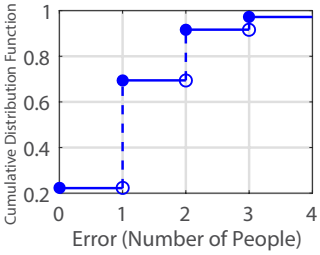

Fig. 8: CDF of the absolute error for head counting in closed areas. It can be seen that our approach can estimate the number of people with a good accuracy.

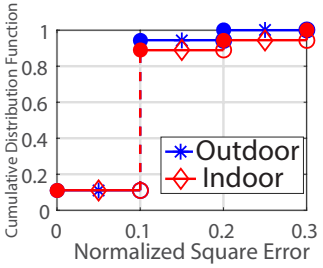

Fig. 9: CDF of the normalized square error for crowd speed estimation as a function of the location. It can be seen that the performance in outdoor and indoor locations are comparable.

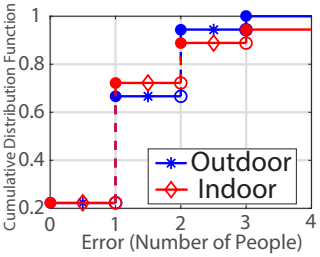

Fig. 10: CDF of the absolute error for head counting as a function of the location. It can be seen that the performance in outdoor and indoor locations are comparable.

error (NMSE) of the speed estimation of all the experiments as 0.046 (i.e., 4.6%) and the mean absolute error (MAE) in estimating the total number of people as 1.3, which further confirms the high accuracy of our proposed system. Fig. 7 and 8 further show the cumulative distribution function (CDF) of the normalized square error (NSE) for speed estimation and the CDF of the absolute error for head counting, respectively. It can be seen that the NSE of speed estimation is less than or equal to 0.1, 92% of the time, and the occupancy estimates are within 1 person error 70% of the time and within 2 people error 92% of the time, thus establishing the robust nature of our proposed system. We further note that the proposed system has a low computational complexity. For instance, it took 0.2 seconds to solve for the case of $N = 20$ and $v = 0.3$. Furthermore, it converges after collecting RSSI measurements for a couple of minutes, with several cases (those with higher speeds) converging in much less than a minute.

We next consider the impact of the environment on the estimation performance. More specifically, Fig. 9 and 10 compare the CDF error curves of the indoor and outdoor areas, for speed estimation and head counting respectively. It can be seen that both the indoor and outdoor areas have similar performances.

To further validate our proposed system in very dense areas with a large number of people, we run a number of experiments where 20 people walked in the area of Fig. 6, with 2 different speeds. As the figure shows, the area can get very crowded when 20 people are present. Table III then shows the performance of our system. It can be seen that our approach

True Arrival Rate and Crowd Speed (λ, v)	Estimated Arrival Rate and Speed in Outdoor Area ($\widehat{\lambda}$, $\widehat{v}$)	Estimated Arrival Rate and Speed in Indoor Area ($\widehat{\lambda}$, $\widehat{v}$)
(0.2, 0.3)	(0.2, 0.4)	(0.22,0.4)
(0.2, 0.8)	(0.16, 0.8)	(0.21, 0.7)
(0.2, 1.6)	(0.15, 1.6)	(0.14, 2.2)
(0.1, 0.3)	(0.1, 0.3)	(0.14, 0.1)
(0.1, 0.8)	(0.1, 1)	(0.1, 1)
(0.1, 1.6)	(0.09, 1.5)	(0.08,2)

TABLE IV: A sample performance of our system when estimating the arrival rate and speed of the people in open areas – the middle and right columns show the performance for the outdoor area of Fig. 4 and indoor area of Fig. 5 respectively, while the left column shows the groundtruth.

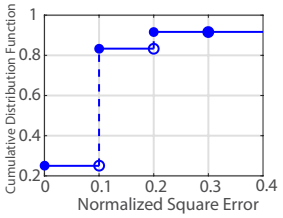

Fig. 11: CDF of the normalized square error for crowd speed estimation in open areas (both indoor and outdoor). It can be seen that our approach can estimate the crowd speed with a good accuracy.

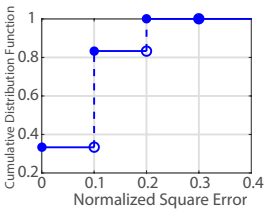

Fig. 12: CDF of the normalized square error for crowd arrival rate estimation in open areas (both indoor and outdoor). It can be seen that our approach can estimate the crowd arrival rate with a good accuracy.

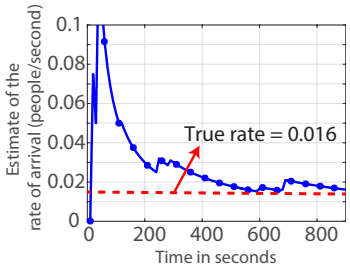

Fig. 13: The estimate of the rate of arrival of people into the aisle of Fig. 14 at Costco, as a function of time. It can be seen that our framework correctly estimates the rate of arrival.

can estimate the occupancy attributes well even when the area is considerably dense.

Open Area: In this section, we validate the performance of our proposed system in open areas. More specifically, we run experiments in the same outdoor and indoor areas of Fig. 4 and 5 but we allow people to enter/exit the area. In other words, people enter the area from one side, walk in the area at the given speed, but with any motion pattern they desire, and then exit the area from the other end. We then run several experiments for different combinations of rate of arrival into the area and walking speed in the area. More specifically, we consider Poisson-distributed arrival times with two rates of 0.2 person/second and 0.1 person/second, and walking speeds of 0.3, 0.8, and 1.6 m/s. Table IV shows the performance of our approach when estimating the arrival rate and speed of a crowd, for both outdoor and indoor areas. It can be seen that the proposed system can accurately estimate the occupancy attributes of an open area. Fig. 11 and 12 further show the CDF of the normalized square error for speed and arrival rate estimation respectively. It can be seen that the NSE of speed estimation is within 0.1, 83% of the time, and the NSE of rate estimation is within 0.2, 100% of the time, thus establishing the robust nature of our proposed system.

1) Costco Experiments: In this section, we use our proposed system to estimate the motion behavior of the buyers in an aisle of a retail store, Costco. Since people constantly come and go through the aisle, this will be an example of the open area scenario. We then estimate the rate of arrival of people into the aisle, and the speed at which people walk while they are exploring the aisle, thus assessing the popularity of the products in the aisle.

Fig. 14 shows the aisle of interest in our local Costco. This aisle contains a specific type of merchandise, snacks and cookies in this case. Both ends of the aisle are open and people can enter/exit from either end of the aisle. It is expected that people walk at a slow pace if the products in the aisle generate interest and they consider buying them. We are thus interested in estimating such behaviors. A pair of WiFi links are located along the aisle, as indicated in Fig. 14, and make wireless measurements as people walk through the aisle. We then use our approach of Section II to estimate the speed of people in the aisle as well as their rate of arrival into the aisle.

More specifically, we collect wireless RSSI measurements

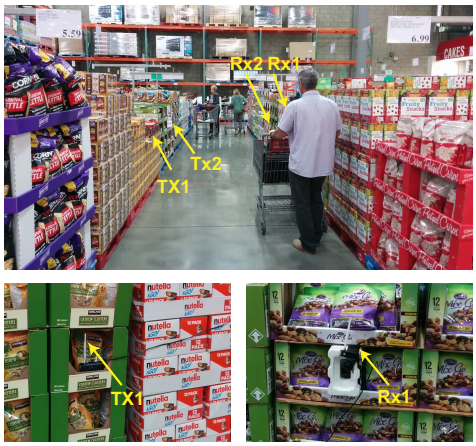

Fig. 14: The Costco experiment – the figure shows the considered "snacks and cookies" aisle in Costco along with a pair of WiFi links positioned along the aisle to make wireless measurements.

for 15 minutes as people walk through the aisle shown in Fig. 14. We manually record the times at which people arrive from either entrance of the aisle, through visual observation since camcording was not allowed, and compute the true rate of arrival. Fig. 13 shows the estimated rate of arrival as a function of time. It can be seen that our framework accurately estimates the rate of arrival of people into the aisle using a pair of WiFi links. Note that the rate of arrival on that particular day/time was 1 person per minute (or 0.016 people/second). Thus, our estimation converges relatively fast, within 400 seconds, which is the time 6 people visited the aisle. Furthermore, the average ground-truth speed of people walking in that aisle is estimated as 0.48 m/s, by manually recording the entrance and exit times of people. The average speed of people walking in the aisle is then estimated as 0.2 m/s using our framework, which is consistent with the ground-truth, and indicates a significant slowdown, showcasing the popularity of the aisle.

Overall, our extensive experiments (total of 51) confirm that the proposed approach can estimate the crowd speed and total number (or arrival rate) robustly and with a high accuracy.

IV. Conclusions

In this paper, we proposed a system to estimate occupancy attributes in an area such as the number of people, walking speed, and the rate of arrival, by using RSSI measurements of a pair of WiFi links, and in a device-free manner. More specifically, we showed how two key statistics, the probability

of crossing and the cross-correlation between the two links, carry key information about the occupancy attributes and mathematically characterized them. To validate our framework, we ran extensive experiments (total of 51) in indoor and outdoor locations, with up to 20 people and with a variety of speeds, and showed that our approach can accurately estimate the occupancy attributes of an area. The NMSE of crowd speed estimation over all the experiments is 0.047, while the NMSE of the arrival rate estimation is 0.034, and the MAE of head counting is 1.3. Finally, we used our framework in Costco, estimated the motion behavior of buyers in an aisle, and deduced the popularity of the products in that aisle.

To the best of our knowledge this is the first time that the speed of a crowd is estimated passively with WiFi signals, or the speed and number of people is jointly estimated for both open and closed areas.

APPENDIX

A. Proof of Theorem 1

Consider a link located in the area of Fig. 1(a), whose x-coordinate is X_i. X_i, for instance, can represent the x-coordinate of either of the links of Fig. 1(a). Let the position of the person at time k be $x(k) \leq X_i$. The person crosses the link at time $k+1$, if she/he chooses a direction $\theta(k)$ at time k such that $x(k) + v\delta t \cos(\theta(k)) \geq X_i$, which results in $|\theta(k)| \leq \cos^{-1}\left(\frac{X_i - x(k)}{v\delta t}\right)$, where $|.|$ is the absolute value of the argument. Since $|\theta(k)| \leq \theta_{\max}$, in order to cross the link, the heading direction has to satisfy $|\theta(k)| \leq \min\left\{\theta_{\max},\ \cos^{-1}\left(\frac{X_i - x(k)}{v\delta t}\right)\right\}$. Since the heading direction is uniformly distributed over μ^d, the probability that a person at $x(k)$ crosses the link at time $k+1$, $p^{x(k)}_{c,\text{singleperson}}$, for $x(k) \leq X_i$, is given by, $p^{x(k)}_{c,\text{singleperson}} = \frac{\min\left\{\theta_{\max},\ \cos^{-1}\left(\frac{X_i - x(k)}{v\delta t}\right)\right\}}{2\theta_{\max}}$. By symmetry, it can be seen that $p^{x(k)}_{c,\text{singleperson}}$, for $x(k) \geq X_i$, is given by, $p^{x(k)}_{c,\text{singleperson}} = \frac{\min\left\{\pi - \theta_{\max},\ \pi - \cos^{-1}\left(\frac{x(k) - X_i}{v\delta t}\right)\right\}}{2\theta_{\max}}$. The probability of crossing the link by a single person, $p_{c,\text{singleperson}}$, is then obtained by summing over all the positions from which a cross can occur:

$$p_{c,\text{singleperson}} = \sum_{x(k)=X_i - v\delta t}^{X_i + v\delta t} \frac{\Delta x}{B} p^{x(k)}_{c,\text{singleperson}}, \tag{9}$$

where $\frac{\Delta x}{B}$ is the probability that a pedestrian is located at any given position in the area. By substituting the expression for $p^{x(k)}_{c,\text{singleperson}}$ in (9) and letting $\delta t \to 0$, we get, $p_{c,\text{singleperson}} = \frac{\int_{X_i - v\delta t}^{X_i + v\delta t} \min\left\{\theta_{\max},\ \cos^{-1}\left(\left|\frac{X_i - x(k)}{v\delta t}\right|\right)\right\} dx}{2B\theta_{\max}}$. By simplifying this further, we get $p_{c,\text{singleperson}} = \frac{v\delta t \sin(\theta_{\max})}{B\theta_{\max}}$, which proves the Theorem.

REFERENCES

[1] J. N. LaPlante and T. P. Kaeser, "The continuing evolution of pedestrian walking speed assumptions," *Institute of Transportation Engineers. ITE Journal*, vol. 74, no. 9, p. 32, 2004.

[2] A. G. Abuarafah, M. O. Khozium, and E. AbdRabou, "Real-time crowd monitoring using infrared thermal video sequences," *Journal of American Science*, vol. 8, no. 3, pp. 133–140, 2012.

[3] P. Liu, S.-K. Nguang, and A. Partridge, "Occupancy inference using pyroelectric infrared sensors through hidden markov models," *IEEE Sensors Journal*, vol. 16, no. 4, pp. 1062–1068, 2016.

[4] Y. Agarwal, B. Balaji, R. Gupta, J. Lyles, M. Wei, and T. Weng, "Occupancy-driven energy management for smart building automation," in *Proceedings of the 2nd ACM Workshop on Embedded Sensing Systems for Energy-Efficiency in Building*. ACM, 2010, pp. 1–6.

[5] F. Wahl, M. Milenkovic, and O. Amft, "A distributed pir-based approach for estimating people count in office environments," in *15th International Conference on Computational Science and Engineering*. IEEE, 2012.

[6] J. Yun and S.-S. Lee, "Human movement detection and identification using pyroelectric infrared sensors," *Sensors*, pp. 8057–8081, 2014.

[7] M. S. Kristoffersen, J. V. Dueholm, R. Gade, and T. B. Moeslund, "Pedestrian counting with occlusion handling using stereo thermal cameras," *Sensors*, vol. 16, no. 1, p. 62, 2016.

[8] B. Yang, J. Luo, and Q. Liu, "A novel low-cost and small-size human tracking system with pyroelectric infrared sensor mesh network," *Infrared Physics & Technology*, vol. 63, pp. 147–156, 2014.

[9] M. Li, Z. Zhang, K. Huang, and T. Tan, "Estimating the number of people in crowded scenes by mid based foreground segmentation and head-shoulder detection," in *19th International Conference on Pattern Recognition, 2008.* IEEE, 2008, pp. 1–4.

[10] S.-F. Lin, J.-Y. Chen, and H.-X. Chao, "Estimation of number of people in crowded scenes using perspective transformation," *IEEE Transactions on Systems, Man, and Cybernetics*, pp. 645–654, 2001.

[11] R. Tomastik, Y. Lin, and A. Banaszuk, "Video-based estimation of building occupancy during emergency egress," in *American Control Conference, 2008*. IEEE, 2008, pp. 894–901.

[12] F. Fleuret, J. Berclaz, R. Lengagne, and P. Fua, "Multicamera people tracking with a probabilistic occupancy map," *IEEE transactions on pattern analysis and machine intelligence*, pp. 267–282, 2008.

[13] M. H. Dridi, "Tracking individual targets in high density crowd scenes analysis of a video recording in hajj 2009," *arXiv preprint arXiv:1407.2044*, 2014.

[14] New CSC Research Reveals Where Shoppers and Retailers Stand on Next Generation In-store Technology, 2015, https://turtl.dxc.technology/story/55ee93d8bbfd077f2d4e22ee.pdf?

[15] New study: consumers overwhelmingly reject in-store tracking by retailers, 2014, https://goo.gl/KfuUQo.

[16] P. Prasertsung and T. Horanont, "How does coffee shop get crowded?: Using WiFi footprints to deliver insights into the success of promotion," in *Proceedings of the 2017 ACM International Joint Conference on Pervasive and Ubiquitous Computing*. ACM, 2017, pp. 421–426.

[17] J. Weppner and P. Lukowicz, "Bluetooth based collaborative crowd density estimation with mobile phones," in *IEEE International Conference on Pervasive Computing and Communications, 2013*, pp. 193–200.

[18] L. M. Ni, Y. Liu, Y. C. Lau, and A. P. Patil, "LANDMARC: Indoor location sensing using active RFID," *Wireless networks*, 2004.

[19] Attention, Shoppers: Store Is Tracking Your Cell, goo.gl/DrZFXW.

[20] Y. Yuan, C. Qiu, W. Xi, and J. Zhao, "Crowd density estimation using wireless sensor networks," in *7th International Conference on Mobile Ad-hoc and Sensor Networks*. IEEE, 2011, pp. 138–145.

[21] C. Xu, B. Firner, R. S. Moore, Y. Zhang, W. Trappe, R. Howard, F. Zhang, and N. An, "SCPL: Indoor device-free multi-subject counting and localization using radio signal strength," in *ACM/IEEE International Conference on Information Processing in Sensor Networks*, 2013.

[22] S. Domenico, M. Sanctis, E. Cianca, and G. Bianchi, "A trained-once crowd counting method using differential WiFi channel state information," in *3rd Intl. Workshop on Physical Analytics*. ACM, 2016.

[23] W. Xi, J. Zhao, X.-Y. Li, K. Zhao, S. Tang, X. Liu, and Z. Jiang, "Electronic frog eye: Counting crowd using wifi," in *IEEE Conference on Computer Communications*. IEEE, 2014, pp. 361–369.

[24] S. Depatla, A. Muralidharan, and Y. Mostofi, "Occupancy estimation using only WiFi power measurements," *IEEE Journal on Selected Areas in Communications*, vol. 33, no. 7, pp. 1381–1393, 2015.

[25] S. Sigg, U. Blanke, and G. Tröster, "The telepathic phone: Frictionless activity recognition from WiFi-RSSI," in *2014 IEEE International Conference on Pervasive Computing and Communications*, pp. 148–155.

[26] S. Shi, S. Sigg, W. Zhao, and Y. Ji, "Monitoring attention using ambient FM radio signals," *IEEE Pervasive Computing*, vol. 13, pp. 30–36, 2014.

[27] M. Bocca, O. Kaltiokallio, N. Patwari, and S. Venkatasubramanian, "Multiple target tracking with RF sensor networks," *IEEE Transactions on Mobile Computing*, vol. 13, no. 8, pp. 1787–1800, 2014.

[28] C. D. Meyer, *Matrix analysis and applied linear algebra*. Siam, 2000.